Chemotherapy-driven dysbiosis in the intestinal microbiome

E. Montassier*,[†], T. Gastinne[‡], P. Vangay[§], G. A. Al-Ghalith[†,§], S. Bruley des Varannes[¶], S. Massart**, P. Moreau[‡], G. Potel*, M. F. de La Cochetière[††], E. Batard* & D. Knights[†,‡‡]

*EA 3826 Thérapeutiques Cliniques et Expérimentales des Infections, Faculté de Médecine, Université de Nantes, Nantes, France.
[†]Department of Computer Science and Engineering, University of Minnesota, Minneapolis, MN, USA.
[‡]Department of Hematology, Nantes University Hospital, Nantes, France.
[§]Biomedical Informatics and Computational Biology, University of Minnesota, Minneapolis, MN, USA.
[¶]Institut des Maladies de l'Appareil Digestif, Nantes University Hospital, Nantes, France.
**Gembloux Agro-Bio Tech, University of Liège, Gembloux, Belgium.
[††]EA 3826 Thérapeutiques Cliniques et Expérimentales des Infections, Faculté de Médecine, INSERM, Université de Nantes, Nantes, France.
[‡‡]BioTechnology Institute, University of Minnesota, St. Paul, MN, USA.

Correspondence to:
Dr. E. Montassier, EA 3826 Thérapeutiques Cliniques et Expérimentales des Infections, Faculté de Médecine, Université de Nantes, 1 Rue G Veil, Nantes 44000, France.
E-mail: emmanuelmontassier@hotmail.com
Prof. D. Knights, Department of Computer Science and Engineering, University of Minnesota, Minneapolis, MN 55455, USA.
E-mail: dknights@umn.edu

SUMMARY

Background
Chemotherapy is commonly used as myeloablative conditioning treatment to prepare patients for haematopoietic stem cell transplantation (HSCT). Chemotherapy leads to several side effects, with gastrointestinal (GI) mucositis being one of the most frequent. Current models of GI mucositis pathophysiology are generally silent on the role of the intestinal microbiome.

Aim
To identify functional mechanisms by which the intestinal microbiome may play a key role in the pathophysiology of GI mucositis, we applied high-throughput DNA-sequencing analysis to identify microbes and microbial functions that are modulated following chemotherapy.

Methods
We amplified and sequenced 16S rRNA genes from faecal samples before and after chemotherapy in 28 patients with non-Hodgkin's lymphoma who received the same myeloablative conditioning regimen and no other concomitant therapy such as antibiotics.

Results
We found that faecal samples collected after chemotherapy exhibited significant decreases in abundances of Firmicutes ($P = 0.0002$) and Actinobacteria ($P = 0.002$) and significant increases in abundances of Proteobacteria ($P = 0.0002$) compared to samples collected before chemotherapy. Following chemotherapy, patients had reduced capacity for nucleotide metabolism ($P = 0.0001$), energy metabolism ($P = 0.001$), metabolism of cofactors and vitamins ($P = 0.006$), and increased capacity for glycan metabolism ($P = 0.0002$), signal transduction ($P = 0.0002$) and xenobiotics biodegradation ($P = 0.002$).

Conclusions
Our study identifies a severe compositional and functional imbalance in the gut microbial community associated with chemotherapy-induced GI mucositis. The functional pathways implicated in our analysis suggest potential directions for the development of intestinal microbiome-targeted interventions in cancer patients.

INTRODUCTION

Chemotherapy is commonly used as myeloablative conditioning treatment to prepare for haematopoietic stem cell transplantation (HSCT).[1] However, chemotherapy leads to several side effects, with gastrointestinal (GI) mucositis being the most frequent in HSCT recipients.[2] GI mucositis is responsible for nonspecific symptoms such as nausea, vomiting, abdominal pain and diarrhoea that are reported in almost all HSCT recipients.[3] Histological GI mucositis lesions are represented by villus atrophy and loss of enterocytes, resulting in epithelium impairment and barrier dysfunction.[4]

A previous model, proposed by Sonis, detailed the pathophysiology of mucositis including: (i) formation of reactive oxygen (ROS), nitrogen (RNS) and sulphur species (RSS) resulting in nuclear factor kappa B activation ($NF\kappa B$), (ii) induction of messenger molecules, such as tumour necrosis factor alpha ($TNF\alpha$) leading to inflammation and apoptosis, (iii) amplification of messenger molecules increasing inflammation and apoptosis and (iv) disruption of the epithelial barrier enabling bacterial translocation.[5] Chemotherapy-induced mucositis often leads to life-threatening systemic infections.[6] However, this previously proposed model does not include the intestinal microbiome, although some studies report microbial changes following chemotherapy.[7] Furthermore, a comprehensive review proposed five pathways through which the intestinal microbiota may impact the pathophysiology of GI mucositis: (i) inflammatory process and oxidative stress, (ii) intestinal permeability, (iii) mucus layer composition, (iv) epithelial repair and (v) production and release of immune effector molecules.[8]

The objective of our study was to perform a high-throughput DNA-sequencing analysis on faecal samples to identify microbial taxa and functions that are modulated following chemotherapy.

MATERIALS AND METHODS

Study patients and faecal sample collection

Participants with non-Hodgkin's lymphoma were recruited in the hematology department of Nantes University Hospital, France. We excluded patients with a history of Inflammatory Bowel Diseases (IBD), were exposed to probiotics, prebiotics or broad-spectrum antibiotics, or were administered nasal-tube feeding or parenteral nutrition in the month prior to initiation of the study. Participants received the same myeloablative conditioning regimen for five consecutive days, including high-dose Carmustine (Bis-chloroethylnitrosourea),

Table 1 | Clinical characteristics of the study population. Participant metadata includes age, sex, body mass index (calculated according to the formula $BMI = W/H^2$, where 'W' is weight in Kilograms, and 'H' is height in metre), use of antibiotic prophylaxis, previous history of chemotherapy and a description of the gastrointestinal (GI) mucositis-related symptoms. Categorical data are reported as percentages and 95% confidence interval (95% CI), and quantitative data are reported as means and median, 1st and 3rd quartile

Clinical features	
Age, years median, 1st and 3rd quartile	55 [45–62]
Sex male, n (%, 95% CI)	18 (64.3, 44.1–80.7)
Body mass index, median, 1st and 3rd quartile	24 [23–27]
Antibiotic prophylaxis, n (%, 95% CI)	24 (85.7, 66.4–95.3)
Penicillin V	14 (50.0, 32.6–67.4)
Cotrimoxazole	18 (64.3, 44.1–80.7)
Cotrimoxazole + penicillin, V	6 (25.0, 10.6–47.0)
Previous history of chemotherapy n (%, 95% CI)	27 (96.4, 79.7–99.8)
GI mucositis-related symptoms n (%, 95% CI)	
Nausea and vomiting	17 (60.7, 40.7–77.8)
Severe Abdominal pain	10 (35.7, 19.3–55.8)
Diarrhoea grade 1 or 2	20 (71.4, 51.1–86.0)
Diarrhoea grade 3 or 4	8 (28.6, 13.9–48.9)

Etoposide, Aracytine and Melphalan. HSCT occurred on Day 7 as reported previously.[9] Most of the participants received antibiotic prophylaxis before the conditioning therapy, based on penicillin V and cotrimoxazole (Table 1). This prophylactic treatment was stopped on the hospital in-patient admission. Therefore, patients did not receive concomitant antibiotics during chemotherapy. We collected two faecal samples from each participant. A faecal sample was collected on hospital in-patient admission (named S1), prior to administration of chemotherapy, and 7 days later immediately prior to HSCT (named S2). For each faecal sample, we collected one gram of stool into a sterile tube subsequently stored at $-80\ °C$ for molecular analysis as previously reported.[9]

16S rRNA gene sequencing

DNA from primary stool samples were extracted with QIAamp DNA Stool Minikit (Qiagen, Hilden, Germany), as previously reported.[9] The aliquots were then stored at $-20\ °C$. We amplified 16S rRNA genes using primers 784F (AGG ATTAGATACCCTGGTA) and 1061R (CRRCACGAGC TGACGAC) targeting the V5 and V6 hypervariable 16S rRNA gene regions.[10] The amplicons were visualised using 1% agarose gels and GelGreen

Nucleic Acid gel stain (Biotium, Hayward, CA, USA) and were then purified using the Wizard® SV Gel and PCR Clean-up System (Promega, Madison, WI, USA). Amplicon DNA concentrations were determined using the Quant-iT PicoGreen dsDNA reagent and kit (Invitrogen, Waltham, MA, USA) and the final concentration of DNA was determined using a NanoDrop spectrophotometer (Thermo Fischer Scientific, Waltham, MA, USA). Pyrosequencing was carried out using primer A on the Roche 454 Life Sciences Genome Sequencer FLX instrument (454 Life Sciences-Roche, Branford, CT, USA) with titanium chemistry at DNAVision (Charleroi, Belgium).

Sequence analysis

The 16S rRNA raw sequences were analysed with the QIIME (Quantitative Insights Into Microbial Ecology) 1.8.0 software.[11] Sequences were assigned to 97% ID OTUs by comparison to the Greengenes reference database 13_8 using pick_open_reference_otus.py.[12] Of the faecal samples collected, a total of 390 773 high-quality 16S rRNA-encoding sequences were identified, representing 4839 OTUs. The median number of sequences obtained per sample was 8524 [6659–10 909]. Since samples contained between 3033 and 24 636 sequences, diversity analyses were rarefied at 3033 sequences per sample to avoid bias. We used the beta_diversity_through_plots.py script to assess the differences in bacterial communities and functional composition between faecal samples collected before and after chemotherapy. We visualised beta diversity using unweighed, weighed UniFrac and Bray–Curtis distances with Principal Coordinate Analysis (PCoA). We used the compare_categories.py script, which applied the ANOSIM method on the previously obtained dissimilarity matrices to determine whether communities differ significantly between faecal samples collected before and after chemotherapy. We used the alpha_rarefaction.py script to compute alpha diversity metrics, which evaluated diversity within a sample and generated rarefaction curves. We then tested differences in alpha diversity between faecal samples collected before and after chemotherapy with a Monte Carlo permuted t-test using the compare_alpha_diversity.py script. We used the supervised_learning.py script and performed Random Forest classification with 500 trees and 10-fold cross-validation to obtain robust estimates of the generalisation error and feature importance.[13] Cross-validation is often used to assess how well a classifier trained on known samples will generalise to a new data set of never before seen samples. To do this, our dataset was partitioned into a training set (including 90% of the patients) and a validation set (including the remaining 10%). The random forest classifier was trained on the 90% and used to predict the outcome of the held out 10%. This was repeated ten times, allowing every patient to act as a test case once. The model's accuracy was determined by its ability on average to predict the outcome of the 10% of patients that were held out. We used the relative abundance in each sample of genera or families as features. The measure of the method's success is its ability to classify new samples as coming from one of the two groups (i.e. faecal sample collected before or after chemotherapy). Random Forests assign an importance score to each genus or family by estimating the increase in error caused by removing that genus from the set of predictors. Here, we considered a genus or a family to be highly predictive if its average importance score was at least 0.001.[14, 15]

Statistical analysis

Quantitative data were reported as medians [25th–75th Percentile]. Qualitative data were reported as percentages [95% confidence interval]. We used PICRUSt, a computational approach to predicting the functional composition of a metagenome using marker gene data (here the 16S rRNA gene) and the Greengenes reference genomes database.[16] Comparison of taxonomic and functional counts data between faecal samples collected before and after chemotherapy were performed using Mann–Withney U test with false discovery rate (FDR) correction for multiple testing. Boxplots, beeswarms and two-dimensional PCoA plots were generated using R.[17] We used a linear model with FDR correction to find associations between clinical data (age, sex, previous antibiotic use, history of chemotherapy and delay of previous chemotherapy) and taxa or predicted functions using code available at https://github.com/danknights/mwas. To find taxa that were resistant to chemotherapy, we used Spearman correlation of within-patient pre- and post-chemotherapy relative abundances, followed by FDR correction. A taxa was considered resistant to chemotherapy if Pearson correlation coefficient >0.70 and FDR-corrected $P < 0.05$). We also computed Pearson correlations between relative abundance of taxa collapsed at genus level and KEGG signalling pathways of L3 categories. We plotted a correlation network of pairs that significantly correlated with a FDR-corrected $P < 0.05$. Network analyses were displayed with Cytoscape using an edge-weighted spring embedded layout.[18] Positive correlations were in blue and negative correlations in grey.

Study approval

Written informed consent was obtained from all patients. The protocol received IRB approval by the Nantes University Hospital Ethics Committee (identification of the protocol: BRD/10/04-Q).

Accession number

Sequences have been deposited on NCBI under BioProject ID PRJNA257960.

RESULTS

Patient and faecal sample characteristics

Twenty-eight patients with non-Hodgkin's lymphoma admitted for HSCT were included in our study. Clinical characteristics of the patients are listed in Table 1. All patients experienced GI mucositis-related symptoms, such as nausea, vomiting, abdominal pain and diarrhoea with varying degrees of severity. Overall, 28 faecal samples were collected before chemotherapy (named S1) and 15 faecal samples were collected after chemotherapy (named S2). Indeed, it was not possible to obtain a faecal sample immediately prior to HSCT in all the patients.

Taxonomic shifts in the microbiome following chemotherapy

PCoA of faecal samples, based on 16S rRNA sequences using the unweighed and weighed UniFrac distance metrics, showed strong differences between faecal samples collected before and after chemotherapy (Figure 1). The

ANOSIM method determined that faecal bacterial communities diverged significantly between samples collected before and after chemotherapy (unweighed UniFrac distance metric: $R = 0.51$, $P = 0.001$; weighted UniFrac distance metric: $R = 0.58$, $P = 0.001$). Moreover, alpha diversity in faecal samples collected after chemotherapy was lower than alpha diversity from samples collected before chemotherapy. The trend is observed with both phylogenetic [Faith's phylogenetic diversity (PD), $P = 0.01$] and nonphylogenetic (observed species, $P = 0.001$) richness metrics (Figure 2). Furthermore, using Random Forest, unknown samples were classified with a 0.09 ± 0.16 error rate, which is 3.7 times better than the baseline error rate for random guessing, showing that faecal microbiota is distinctly altered following chemotherapy. Thus, faecal microbiota of patients that received high-dose chemotherapy conditioning HSCT exhibited a rapid and marked decreased overall diversity.

At the phylum level, faecal samples collected after chemotherapy exhibited significant decreases in abundances of Firmicutes (Mann–Whitney U test, FDR-corrected $P = 0.0002$) and Actinobacteria (Mann–Whitney U test, FDR-corrected $P = 0.002$) and significant increases in abundances of Proteobacteria (Mann–Whitney U test, FDR-corrected $P = 0.0002$) compared to samples collected before chemotherapy (Table S1a, Figure 3a). At the genus level, we found that faecal samples collected after chemotherapy exhibited significantly decreased abundance in *Ruminococcus, Oscillospira, Blautia, Lachnospira, Roseburia, Dorea, Coprococcus, Anaerostipes, Clostridium, Collin-*
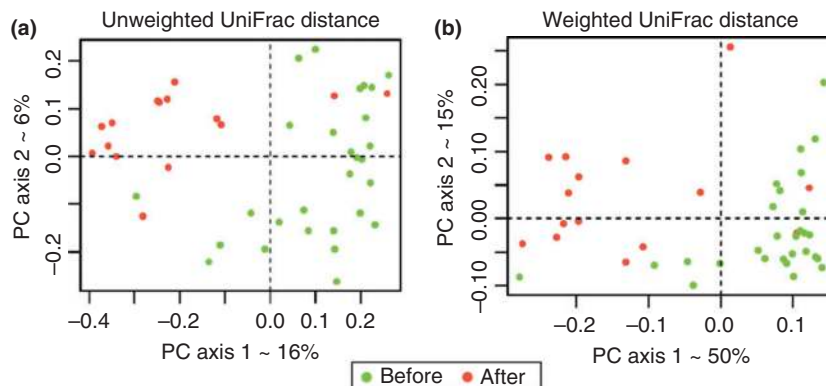

Figure 1 | Beta-diversity comparisons of the gut microbiomes of the faecal samples collected before chemotherapy and after chemotherapy. Analyses were performed on 16S rRNA V5 and V6 regions data, with a rarefaction depth of 3033 reads per sample. (a) Principal Coordinate Analysis (PCoA) of unweighted UniFrac distances. Proportion of variance explained by each principal coordinate axis is denoted in the corresponding axis label. (b) Principal Coordinate Analysis (PCoA) of weighted UniFrac distances. Proportion of variance explained by each principal coordinate axis is denoted in the corresponding axis label. The PCoAs shows clear separation between faecal samples collected before chemotherapy and after chemotherapy.
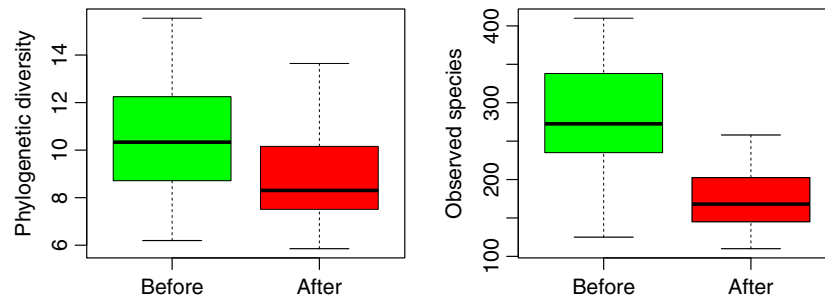
Figure 2 | Alpha-diversity comparisons of the gut microbiomes of the faecal samples collected before chemotherapy and after chemotherapy. Analyses were performed on 16S rRNA V5 and V6 regions data, with a rarefaction depth of 3033 reads per sample. Whiskers in the boxplot represent the range of minimum and maximum alpha diversity values within a population, excluding outliers. Alpha diversity in faecal samples collected after chemotherapy was lower than alpha diversity from samples collected before chemotherapy as observed with both phylogenetic (Faith's phylogenetic diversity (PD), $P = 0.01$) and nonphylogenetic (observed species, $P = 0.001$) richness metrics.

sella, *Adlercreutzia* and *Bifidobacterium* compared to samples collected before chemotherapy (Mann–Whitney *U* test, FDR-corrected $P < 0.05$). Moreover, samples collected after chemotherapy exhibited significantly increased abundance in *Citrobacter*, *Klebsiella*, *Enterococcus*, *Megasphaera* and *Parabacteroides* compared with samples collected before chemotherapy (Mann–Whitney *U* test, FDR-corrected $P < 0.05$, Table S1 b–d, Figure 3b).

We also found that *Actinomyces*, *Mobiluncus*, *Scardovia*, *Slackia*, *Prevotella*, *Mitsuokella*, *Oxalobacter* and Erysipelotrichaceae significantly correlated before and after chemotherapy (Pearson correlation coefficient >0.70, FDR-corrected $P < 0.05$) and were therefore considered to be resistant to chemotherapy (Table S2, Figure S1). Thus, faecal microbiota of patients that received high-dose chemotherapy conditioning HSCT exhibited a distinct disruption in bacterial composition.

Moreover, to elucidate the effect of the discontinuation of antibiotics, which are stopped the day before admission to the hospital in our study, and the effect of the chemotherapy, we compare changes in the microbiome observed in our study to a previous study that applied two courses of antibiotics separated by an interval of 6 months.[19] As samples were collected daily for two 19-day periods surrounding each antibiotic course, we analysed the faecal sample collected the day after the antibiotic discontinuation (corresponding to our first faecal sample collected on hospital in-patient admission on the day after antibiotic discontinuation) and a faecal sample collected 7 days after the antibiotic discontinuation (corresponding to our second faecal sample, collected 7 days after hospital in-patient admission, that is 7 days after antibiotic discontinuation). Therefore, we can compare the microbiome changes in the two popula-

tions, and calculate taxonomic abundance ratios between the faecal samples collected 7 days after antibiotic discontinuation and samples collected the day after antibiotic discontinuation. The comparison of these ratios at phylum level suggested that in our study, the results of the discontinuation of the antibiotic are minor as compared with the effect of the chemotherapy. Indeed, there is some divergence between the Dethlefsen and Relman study [19] and our study; the Firmicutes to Bacteroides ratio is low in ours but high in theirs (Figure S2).

Functional shifts in the microbiome following chemotherapy

We found larger overall shifts in microbial functions (42% of all analysed KEGG signalling pathways of L3 categories) compared to shifts in microbial taxa (20% of all analysed genera) after chemotherapy. PCoA of faecal samples based on predicted functions using the Bray–Curtis distance metric showed strong differences between samples collected before and after chemotherapy (Figure 4). The ANOSIM method determined that the faecal microbiome diverged significantly between samples collected before and after chemotherapy (Bray–Curtis distance metric: $R = 0.54$, $P = 0.01$). Procrustes analysis of Bray–Curtis principal coordinate matrices showed concordance between microbes and microbial functions in faecal samples collected before chemotherapy (M2 = 0.59, Monte Carlo $P < 0.001$, Figure S3a) and in faecal samples collected after chemotherapy (M2 = 0.45, Monte Carlo $P < 0.001$, Figure S3b).

Collectively, amino acid metabolism (FDR-corrected $P = 0.004$), nucleotide metabolism (FDR-corrected $P = 0.0001$), energy metabolism (FDR-corrected $P = 0.001$), metabolism of cofactors and vitamins (FDR-corrected
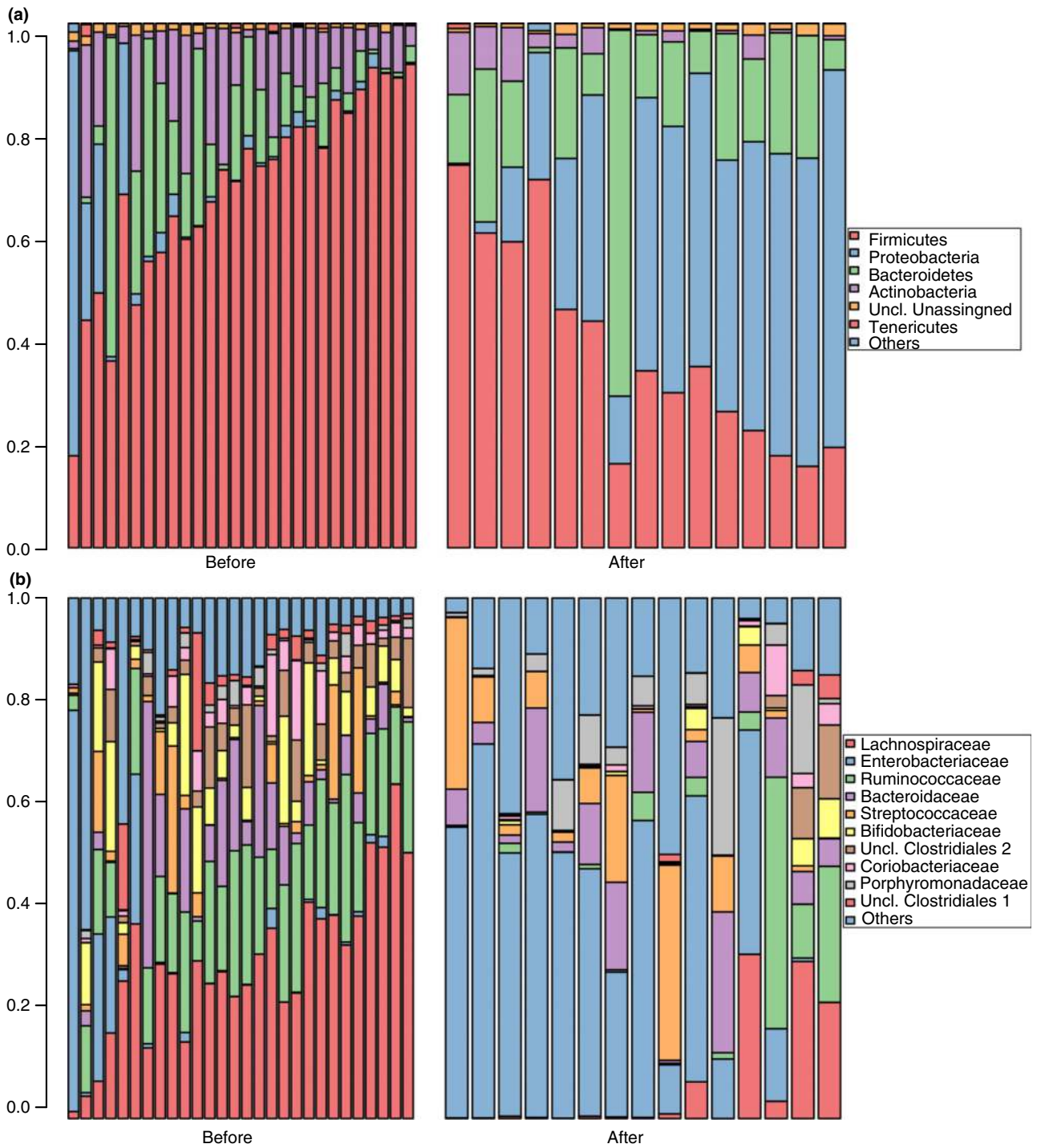
Figure 3 | Taxonomic profile of the gut microbiomes of the samples collected before and after chemotherapy. Analyses were performed on 16S rRNA V5 and V6 regions data, with a rarefaction depth of 3033 reads per sample. (a) Relative taxa abundance plots for individuals from the samples collected before and after chemotherapy, summarised at the phylum level. Individuals are represented along the horizontal axis, and relative taxa frequency is denoted by the vertical axis. (b) Relative taxa abundance plots for individuals from the samples collected before and after chemotherapy, summarised at the family level. Individuals are represented along the horizontal axis, and relative taxa frequency is denoted by the vertical axis.
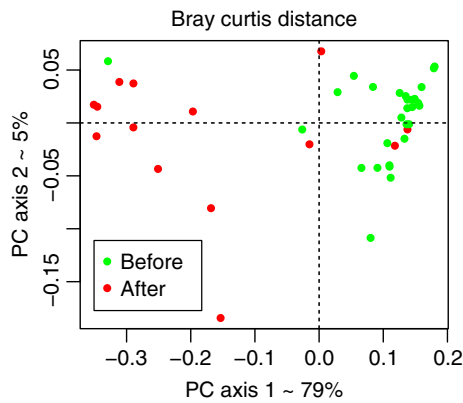
Figure 4 | Functional diversity of the gut microbiomes of the faecal samples collected before chemotherapy and after chemotherapy. Principal Coordinates Analysis of Bray–Curtis distances generated from KEGG Orthologue tables rarefied to 200 000 counts per sample. Proportion of variance explained by each principal coordinate axis is denoted in the corresponding axis label. The PCoA shows clear separation between faecal samples collected before chemotherapy and after chemotherapy.

$P = 0.006$) and carbohydrate metabolism (FDR-corrected $P = 0.20$) categories were decreased in samples collected after chemotherapy compared to samples collected before chemotherapy. In contrast, signal transduction (FDR-corrected $P = 0.0002$), xenobiotics biodegradation (FDR-corrected $P = 0.002$) and glycan metabolism (FDR-corrected $P = 0.0002$) categories were enriched in samples collected after chemotherapy compared to samples collected before chemotherapy (Figure 5, Table S3a). Interestingly, these modulated pathways were similar to those found in a recent study differentiating remission and active colitis in mice.[20]

We also found an enrichment in sulphur, nitrogen, glutathione, riboflavin metabolism and phosphotransferase system in samples collected after chemotherapy (Figure S4, Table S3b), as found in mice with colitis and in IBD patients.[21, 22] The thiamine metabolism pathway, as previously reported in Crohn's disease (CD) patients, was reduced following chemotherapy.[23] Following chemotherapy, within the cell motility category, we found an increase in bacterial motility proteins and flagellar assembly (Figure S4, Table S3b), as found in mice with active acute colitis.[20] Flagella are essential for bacterial pathogenesis, and are required for bacterial motility, adhesion, invasion and secretion of virulence factors.[24, 25]

Within the xenobiotics biodegradation category, most of the pathways were increased following chemotherapy

(Figure S4, Table S3b). Aminobenzoate degradation was previously associated with disease and fluorobenzoate degradation with disease severity in CD patients. Benzoate also promotes Enterobacteriaceae growth and virulence.[26, 27] Moreover, following chemotherapy, we found an increase in pathways involved in pathogenesis and virulence processes (bacterial secretion system, secretion system and adherence/invasion) as found in CD patients and in mice with acute colitis.[21, 22] These pathways are implicated in the secretion of cell wall-degrading enzymes and toxins, inducing epithelium impairment and barrier dysfunction.[28, 29] Nine microbial functions in the replication and repair categories were depleted after chemotherapy, indicating a decreased ability for epithelial repair.

Network analyses of taxonomic and functional repertoire

In samples collected before chemotherapy, we found 35 taxon-functional pathway pairs that were significantly correlated and, in samples collected after chemotherapy, we found 33 taxon-functional pathway pairs that were significantly correlated ($q < 0.05$), both at the family level.

In samples collected before chemotherapy, the correlation network consisted of 43 nodes (taxa or functional pathways) and 95 edges (correlations) (Figure S5a, Table S4a). These correlations mostly implicated Firmicutes and Bacteroidetes. Members of Firmicutes were negatively correlated with cell motility, glycan metabolism and xenobiotic degradation, pathways that were previously associated with intestinal inflammation.[20, 21, 23] In contrast, Clostridiales was positively correlated with amino acid metabolism, as well as members of Bacteroidetes. Members of Bacteroidetes were also negatively correlated with xenobiotics biodegradation and membrane transport, pathways linked to intestinal inflammation.[20, 20, 23] Moreover, *Faecalibacterium* was negatively correlated with glutathione metabolism and phosphotransferase system, pathways associated with oxidative stress, and *Ruminococcus* was positively correlated with carbohydrate metabolism, a pathway associated with protection against intestinal inflammation in mice and humans.[20, 30, 31]

In samples collected after chemotherapy, the network consisted of 35 nodes and 113 edges (Figure S5b, Table S4b). This post-chemotherapy network showed increased correlation implicating phylum Proteobacteria (94% increase as compared to samples collected before chemotherapy). Firmicutes members were negatively correlated
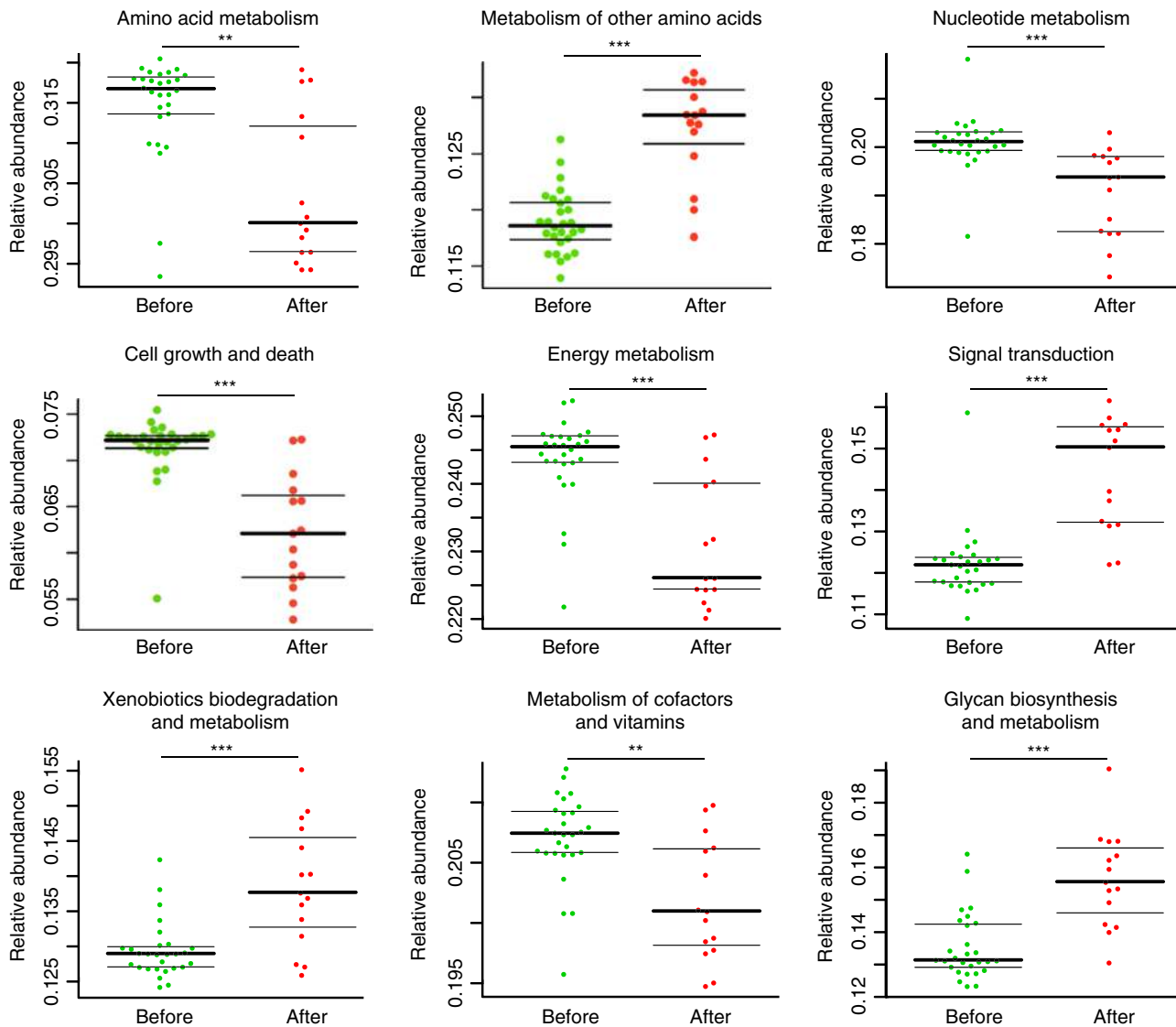
Figure 5 | Relative abundance of the most significant metabolic pathways (L2 KEGG Orthology profiles) in samples collected before ($n = 28$) and after chemotherapy ($n = 15$) Mann–Whitney test: *$P < 0.05$; **$P < 0.01$ and ***$P < 0.001$. Boxplots denote top quartile, median and bottom quartile.

with glycan metabolism and signal transduction, pathways that were previously associated with intestinal inflammation.[20, 21, 23] In contrast, *Enterobacteriaceae* was negatively correlated with enzyme families, metabolism of nearly all amino acids and nucleotide metabolism, pathways previously associated with healthy states; and was positively correlated with signal transduction, xenobiotics degradation, membrane transport, cell motility, riboflavin, glutathione, nitrogen and sulphur metabolism, all pathways known to be associated with intestinal inflammation.[20, 21, 23] Thus, these network analyses reinforce the findings that a specific imbalance in taxonomic composition and metabolic capacity is

associated with intestinal inflammation, as previously characterised in various acute and chronic intestinal inflammation states in mice and humans.

DISCUSSION

Microbiome-targeted studies aim to shed light on the composition and function of the intestinal microbiome in multiple disease conditions.[32] Here, we identified microbes and microbial functions that change following chemotherapy using 16S rRNA high-throughput sequencing-based approaches. As all the patients in our cohort experienced GI mucositis symptoms after chemotherapy, our study provided new insights into intestinal

microbiome changes that may be implicated in the chemotherapy-induced GI mucositis pathophysiology. We identified microbes and microbial functions that may be useful for the development of future microbiome-targeted therapies to manage GI mucositis in cancer patients.

We confirmed that chemotherapy was associated with reduced diversity, as previously reported.[9] Reduced richness of the intestinal microbiota is a well-described feature of intestinal inflammation as found in obese or elderly patients, as well as patients with HIV or IBD.[15, 33–35]

Our study identified microbes that changed during chemotherapy independently of covariates such as age, sex, previous history of antibiotic use and previous history of chemotherapy. Samples collected after chemotherapy were marked with an increased in Enterococcaceae and Enterobacteriaceae, and a decrease in Firmicutes (Ruminococcaceae, Lachnospiraceae) and Actinobacteria (*Bifidobacterium*), among others. These findings extend those reported in the literature.[7] Recently, a study in mice observed that a substantial decrease in the absolute number and diversity of bacterial species was associated with an increase in potentially enteropathogenic bacteria such as *Bacteroides*, Enterococci and Enterobacteriaceae following methotrexate administration.[36]

Our study also identified metabolic pathways that changed during chemotherapy. Amino acid metabolism, carbohydrate metabolism, nucleotide metabolism, energy metabolism, and metabolism of cofactors and vitamins categories were decreased in samples collected after chemotherapy compared to samples collected before chemotherapy, whereas signal transduction, xenobiotics biodegradation and glycan metabolism categories were enriched in samples collected after chemotherapy compared with samples collected before chemotherapy. An intestinal microbiome enriched for glycan metabolism and depleted for amino-acid and carbohydrate metabolism, as found after chemotherapy in our study, was previously associated with intestinal inflammation in human and mouse models (Table S5).[21, 30] As short chain fatty acids (SCFAs) contributed to host energy homeostasis, the intestinal microbiome following chemotherapy is associated with limited capacity for energy harvest.[37] Moreover, increased nitrogen and sulphur pathways during chemotherapy reflect inflammatory processes and production of specific metabolites (ROS, RNS, RSS) under oxidative stress conditions and glutathione and riboflavin pathways, also increased following

chemotherapy, were increased in inflammatory diseases in human and mouse models, and were positively correlated with inflammation and bacterial translocation in HIV patients (Table S5).[21, 38–40] These increases may represent the intestinal microbiome attempt to resist oxidative stress.[21] Furthermore, following chemotherapy, we found an increase in bacterial motility proteins, flagellar assembly and an increase in signal transduction pathway, which were previously associated with inflammatory environment (Table S5).[24, 25, 41]

Van Vliet *et al.* previously proposed that microbiota may play a role in the pathophysiology of GI mucositis.[8] We now discuss our observations of chemotherapy-modulated microbes and microbial functions in the context of the current understanding of the pathophysiology of GI mucositis, specifically the five pathophysiological phases proposed by Sonis mentioned above.[5] First, the intestinal microbiome may modulate the activation of NFκB and the induction of TNFα, potentially favouring inflammation. Several taxa that we found decreased after chemotherapy, such as *Faecalibacterium*, *Ruminococcus*, *Coprococcus*, *Dorea*, *Lachnospira*, *Roseburia* and *Clostridium*, are well-known to diminish inflammation by modulation of the NFκB pathway.[42] *Bifidobacterium*, which was decreased following chemotherapy, also has the ability to inhibit inflammation in intestinal epithelial cells through attenuation of TNFα and lipopolysaccharide-induced inflammatory responses.[43, 44] Moreover, several taxa depleted following chemotherapy in our study (*Roseburia*, *Coprococcus*, *Bifidobacterium*, *Ruminococcus*, *Faecalibacterium*) are butyrate-producing bacteria, resulting in reduced production of SCFAs, well-described to maintain the homeostasis in the colonic mucosa and inhibit inflammatory response.[8, 45] Moreover, *Citrobacter*, found increased after chemotherapy in our study, has the ability to activate NFκB and therefore may increase inflammatory responses.[46] Globally, Enterobacteriaceae were increased after chemotherapy in our study, similar to that of IBD and an active colitis mouse model.[20, 21, 47] Furthermore, the thiamine pathway, found decreased after chemotherapy in our study, was negatively correlated with inflammation in cancer patients and its anti-inflammatory properties have been well-described in mammals.[23, 48, 49] The lipopolysaccharide (LPS) biosynthesis pathway, found to be increased after chemotherapy in our study, possibly increases intestinal inflammation.[50] In our study, we also found that nitrogen and sulphur metabolisms were increased after chemotherapy, extending the link between oxidative stress and increased Enterobacteriaceae (Figure S6).

Second, the intestinal microbiome may modulate intestinal permeability.[51–54] TNFα and NFκB have the ability to increase the production of myosin light-chain kinase resulting in the disorganisation of tight-junction proteins. Indeed, depleted *Faecalibacterium, Ruminococcus, Coprococcus, Dorea, Lachnospira, Roseburia, Clostridium* and *Bifidobacterium* after chemotherapy were associated with increased intestinal permeability through NFκB and TNFα inhibition.[55] Colonisation of the GI tract with *Bifidobacterium* reduces intestinal endotoxin formation.[56] Moreover, *Bifidobacterium infantis* Y1 was able to increase the production of tight-junction proteins and transepithelial resistance, which reduces colonic permeability.[57] Thus, a decrease in *Bifidobacterium* after chemotherapy, as found in our study, may be detrimental to the maintenance of efficient barrier function. A decreased in butyrate-producing bacteria after chemotherapy also reduces intestinal permeability and leads to barrier dysfunction.[58] Furthermore, previous studies reported that LPS-induced inflammation increased intestinal permeability through TLR-4-dependent up-regulation of CD14 membrane expression.[50, 59–61] The increase in the glycosaminoglycan degradation pathway after chemotherapy revealed that microbes degrade glycosaminoglycan, which may deteriorate the intestinal barrier, as found in mice.[62] The increased pathways implicated in pathogenesis and virulence processes (bacterial secretion system, secretion system and adherence/invasion) following chemotherapy may also resulted in intestinal epithelial barrier dysfunction.[28, 29]

Third, the intestinal microbiome may modulate the composition of the mucus layer. Butyrate-producing bacteria play a role in the composition of the mucus layer, as butyrate has the ability to increase mucin synthesis via MUC2.[63] Therefore, the reduction in butyrate-producing bacteria after chemotherapy may be detrimental to the mucus layer composition, potentially leading to tissue damage and translocation of bacteria.[37] The mucus layer may also be compromised by specific pathogens, such as *Enterobacteriaceae*, which can form biofilms on the epithelial surface that alter the mucus layer.[64] Moreover, mucin synthesis may be altered by the limited availability of some amino acids. Specifically, the decrease in cysteine, proline and methionine metabolism following chemotherapy may be responsible for decreased mucin synthesis and impaired colonic protection.[65, 66] Another study demonstrated that L-cysteine and methylmethionine sulfonium chloride inhibited ethanol-induced gastric mucosal damage and increased the

amount of surface mucin in rats.[67] Furthermore, *Citrobacter*, found increased after chemotherapy in our study, may participate in the degradation of the mucus barrier, using mucinases or glycosidases to digest mucin.[68] Adding rectal mucosal samples to future studies would likely improve our ability to understand histological and mucosa-associated microbiota changes. However, in a fragile population of cancer patients receiving a high dose of chemotherapy the infectious risk of such a procedure is generally considered too high.

On the basis of our findings, we proposed that the taxonomic and functional dysbiosis found after chemotherapy may be implicated in the pathophysiology of GI mucositis (Figure S6). The intestinal microbiome after chemotherapy was associated with increased capacity for promoting colonisation, and invasion of mucosa and host systemic organs. This may favour bacterial translocation in these immunocompromised patients.[5] Bloodstream infections (BSI) are a frequent complication in cancer patients receiving chemotherapy.[6, 69] In previous studies, the incidence of BSI was reported to be 22–62%.[70–73] In many cases, the infection enters the bloodstream from the digestive tract, as the lining of the digestive tract is severely compromised.[70, 72, 73] Importantly, sepsis-associated mortality ranges from 9% to 31% in HSCT patients.[70, 72, 73]

CONCLUSIONS

In summary, we found a profound disruption of the intestinal microbiome in terms of both taxonomic composition and metabolic capacity that may partly explain the acute inflammation, known as GI mucositis, observed after chemotherapy. This dysbiosis is also characteristic of other acute and chronic inflammatory conditions in mice as well as in humans, suggesting a causal role for the microbiome in chemotherapy-induced GI mucositis. Therefore, interventions targeting taxonomic and functional imbalances may be relevant to limiting the burden of HSCT-related complications and to reducing the cost of care.

AUTHORSHIP

and interpreted the data. E.M., T.G., P.M. and E.B. conceived and designed the study.

All authors have approved the final version of the article, including the authorship list.

ACKNOWLEDGEMENTS

SUPPORTING INFORMATION

Additional Supporting Information may be found in the online version of this article:

Figure S1. Scatter plot of taxa that significantly correlate before and after chemotherapy (i.e. taxa that are resistant to chemotherapy). Analyses were performed on 16S rRNA V5 and V6 regions data, with a rarefaction depth of 3033 reads per sample. OTUs were collapsed to the genus level. We performed Spearman correlation of taxon–taxon relative abundance and included only those links with correlation >0.7 and FDR-corrected $P < 0.05$.

Figure S2. Scatter plot of the ratio of taxa collapsed at phylum level, after antibiotic discontinuation in Dethlefsen and Relman study (x label) and our study (y label).[19] The ratio was built between the fist sample collected the day after the antibiotic discontinuation and a sample collected 7 days later. We compared the microbiome changes in the two populations, and calculated taxonomic abundance ratios between the faecal samples collected 7 days after antibiotic discontinuation and samples collected the day after antibiotic discontinuation. The comparison of these ratios at phylum level suggested that in our study, the results of the discontinuation of the antibiotic are minor as compared with the effect of the chemotherapy. Indeed, there is some divergence between the Dethlefsen and Relman study [19] and our study, the Firmicutes to Bacteroides ratio is low in ours but high in theirs.

Figure S3. (a) Procrustes analyses comparing spatial fit of Bray–Curtis principal coordinate matrices of microbes (blue points, $n = 28$) and microbial functions (red points, $n = 28$) in faecal samples collected before chemotherapy. (b) Procrustes analyses comparing spatial fit of Bray–Curtis principal coordinate matrices of microbes (blue points, $n = 15$) and microbial functions (red points, $n = 15$) in faecal samples collected before chemotherapy. These analyses showed concordance in faecal samples collected before chemotherapy and after

chemotherapy, indicating consistency between taxonomic and functional profiles ($P < 0.001$ in both cases).

Figure S4. Relative abundance of the most significant metabolic pathways (L3 KEGG Orthology profiles) in samples collected before ($n = 28$) and after chemotherapy ($n = 15$) Mann–Whitney test: *$P < 0.05$; **$P < 0.01$ and ***$P < 0.001$. Boxplots denote top quartile, median and bottom quartile.

Figure S5. Correlation network including OTUs collapsed at genus level and KEGG Orthology profiles in faecal samples collected before chemotherapy (a) and in samples collected after chemotherapy (b). Positive correlations are in blue and negative correlations are in grey. Nodes are positioned using an edge-weighted spring embedded layout.

Figure S6. Proposed pathophysiology of chemotherapy-induced mucositis incorporating the role of the intestinal microbiome.

Table S1. (a) Phyla that discriminated faecal microbiota from faecal samples collected before chemotherapy and faecal samples collected after chemotherapy (Mann–Whitney U test, false discovery rate (FDR)-corrected $P < 0.05$). (b) Families that discriminated faecal microbiota from faecal samples collected before chemotherapy and faecal samples collected after chemotherapy (Mann–Whitney U test, FDR-corrected $P < 0.05$). (c) Genera that discriminated faecal microbiota from faecal samples collected before chemotherapy and faecal samples collected after chemotherapy (Mann–Whitney U test, FDR-corrected $P < 0.05$). (d) Association using a linear model of clinical covariates and taxonomic data collapsed at genus level.

Table S2. Taxa that significantly correlate before and after chemotherapy, (i.e. taxa that are resistant to chemotherapy). We used Spearman correlation of within-patient pre- and post-chemotherapy relative abundances. Taxa that are resistant to chemotherapy are those with a Pearson correlation coefficient >0.70 and a false discovery rate (FDR)-corrected $P < 0.05$.

Table S3. (a) L2 KEGG signalling pathways that discriminated faecal microbiota from faecal samples collected before chemotherapy and faecal samples collected after chemotherapy (Mann–Whitney U test, false discovery rate (FDR)-corrected $P < 0.25$). (b) L3 KEGG signalling pathways that discriminated faecal microbiota from faecal samples collected before chemotherapy and faecal samples collected after chemotherapy (Mann–Whitney U test, false discovery rate (FDR)-corrected $P < 0.25$).

Table S4. (a) Correlation network in samples collected before chemotherapy, at family level and KEGG signalling pathways of L2 categories. Spearman correlation,

false discovery rate (FDR)-corrected *P* value. (b) Correlation network in samples collected after chemotherapy, at family level and KEGG signalling pathways of L2 categories. Spearman correlation, false discovery rate (FDR)-corrected *P* value.

Table S5. Metabolic pathways that changed during acute and chronic inflammation, in mice and humans published in recent datasets. Microbial functions that changed in the same direction in more than 2 datasets are highlighted in yellow.

REFERENCES

1. Vose JM, Anderson JR, Kessinger A, *et al.* High-dose chemotherapy and autologous hematopoietic stem-cell transplantation for aggressive non-Hodgkin's lymphoma. *J Clin Oncol* 1993; **11**: 1846–51.
2. Elting LS, Cooksley C, Chambers M, Cantor SB, Manzullo E, Rubenstein EB. The burdens of cancer therapy. Clinical and economic outcomes of chemotherapy-induced mucositis. *Cancer* 2003; **98**: 1531–9.
3. Blijlevens NMA, Lutgens LCHW, Schattenberg AVMB, Donnelly JP. Citrulline: a potentially simple quantitative marker of intestinal epithelial damage following myeloablative therapy. *Bone Marrow Transplant* 2004; **34**: 193–6.
4. Keefe DM, Brealey J, Goland GJ, Cummins AG. Chemotherapy for cancer causes apoptosis that precedes hypoplasia in crypts of the small intestine in humans. *Gut* 2000; **47**: 632–7.
5. Sonis ST. The pathobiology of mucositis. *Nat Rev Cancer* 2004; **4**: 277–84.
6. Marin M, Gudiol C, Ardanuy C, *et al.* Bloodstream infections in neutropenic patients with cancer: differences between patients with haematological malignancies and solid tumours. *J Infect* 2014; **69**: 417–23.
7. Touchefeu Y, Montassier E, Nieman K, *et al.* Systematic review: the role of the gut microbiota in chemotherapy- or radiation-induced gastrointestinal mucositis - current evidence and potential clinical applications. *Aliment Pharmacol Ther* 2014; **40**: 409–21.
8. Van Vliet MJ, Harmsen HJM, de Bont ESJM, Tissing WJE. The role of intestinal microbiota in the development and severity of chemotherapy-induced mucositis. *PLoS Pathog* 2010; **6**: e1000879.
9. Montassier E, Batard E, Massart S, *et al.* 16S rRNA gene pyrosequencing reveals shift in patient faecal microbiota during high-dose chemotherapy as conditioning regimen for bone marrow transplantation. *Microb Ecol* 2014; **67**: 690–9.
10. Andersson AF, Lindberg M, Jakobsson H, Bäckhed F, Nyrén P, Engstrand L. Comparative analysis of human gut microbiota by barcoded pyrosequencing. *PLoS ONE* 2008; **3**: e2836.
11. Caporaso JG, Kuczynski J, Stombaugh J, *et al.* QIIME allows analysis of high-throughput community sequencing data. *Nat Methods* 2010; **7**: 335–6.
12. DeSantis TZ, Hugenholtz P, Larsen N, *et al.* Greengenes, a chimera-checked 16S rRNA gene database and workbench compatible with ARB. *Appl Environ Microbiol* 2006; **72**: 5069–72.
13. Knights D, Costello EK, Knight R. Supervised classification of human microbiota. *FEMS Microbiol Rev* 2011; **35**: 343–59.
14. Yatsunenko T, Rey FE, Manary MJ, *et al.* Human gut microbiome viewed across age and geography. *Nature* 2012; **486**: 222–7.
15. Lozupone CA, Li M, Campbell TB, *et al.* Alterations in the gut microbiota associated with HIV-1 infection. *Cell Host Microbe* 2013; **14**: 329–39.
16. Langille MGI, Zaneveld J, Caporaso JG, *et al.* Predictive functional profiling of microbial communities using 16S rRNA marker gene sequences. *Nat Biotechnol* 2013; **31**: 814–21.
17. Team RC. R: a Language and Environment for Statistical Computing (R Foundation for Statistical Computing, 2012) ISBN 3-900051-07-0.
18. Saito R, Smoot ME, Ono K, *et al.* A travel guide to Cytoscape plugins. *Nat Methods* 2012; **9**: 1069–76.
19. Dethlefsen L, Relman DA. Incomplete recovery and individualized responses of the human distal gut microbiota to repeated antibiotic perturbation. *Proc Natl Acad Sci USA* 2011; **108**: 4554–61.
20. Rooks MG, Veiga P, Wardwell-Scott LH, *et al.* Gut microbiome composition and function in experimental colitis during active disease and treatment-induced remission. *ISME J* 2014; **8**: 1403–17.
21. Morgan XC, Tickle TL, Sokol H, *et al.* Dysfunction of the intestinal microbiome in inflammatory bowel disease and treatment. *Genome Biol* 2012; **13**: R79.
22. Schwab C, Berry D, Rauch I, *et al.* Longitudinal study of murine microbiota activity and interactions with the host during acute inflammation and recovery. *ISME J* 2014; **8**: 1101–14.
23. Gevers D, Kugathasan S, Denson LA, *et al.* The treatment-naive microbiome in new-onset Crohn's disease. *Cell Host Microbe* 2014; **15**: 382–92.
24. Ottemann KM, Miller JF. Roles for motility in bacterial-host interactions. *Mol Microbiol* 1997; **24**: 1109–17.
25. Ramos HC, Rumbo M, Sirard J-C. Bacterial flagellins: mediators of pathogenicity and host immune responses in mucosa. *Trends Microbiol* 2004; **12**: 509–17.
26. Lyte M, Vulchanova L, Brown DR. Stress at the intestinal surface: catecholamines and mucosa-bacteria interactions. *Cell Tissue Res* 2011; **343**: 23–32.
27. Freestone PPE, Walton NJ, Haigh RD, Lyte M. Influence of dietary catechols on the growth of enteropathogenic bacteria. *Int J Food Microbiol* 2007; **119**: 159–69.
28. Jha G, Rajeshwari R, Sonti RV. Bacterial type two secretion system secreted proteins: double-edged swords for plant pathogens. *Mol Plant Microbe Interact* 2005; **18**: 891–8.
29. Sandkvist M. Type II secretion and pathogenesis. *Infect Immun* 2001; **69**: 3523–35.
30. Tong M, McHardy I, Ruegger P, *et al.* Reprograming of gut microbiome energy metabolism by the FUT2 Crohn's disease risk polymorphism. *ISME J* 2014; **8**: 2193–206.
31. De Fazio L, Cavazza E, Spisni E, *et al.* Longitudinal analysis of inflammation and microbiota dynamics in a model of mild chronic dextran sulfate sodium-induced colitis in mice. *World J Gastroenterol* 2014; **20**: 2051–61.
32. Huttenhower C, Knight R, Brown CT, *et al.* Advancing the microbiome research community. *Cell* 2014; **159**: 227–30.

33. Manichanh C, Rigottier-Gois L, Bonnaud E, et al. Reduced diversity of faecal microbiota in Crohn's disease revealed by a metagenomic approach. Gut 2006; 55: 205–11.

34. Turnbaugh PJ, Hamady M, Yatsunenko T, et al. A core gut microbiome in obese and lean twins. Nature 2009; 457: 480–4.

35. Claesson MJ, Jeffery IB, Conde S, et al. Gut microbiota composition correlates with diet and health in the elderly. Nature 2012; 488: 178–84.

36. Fijlstra M, Ferdous M, Koning AM, Rings EHHM, Harmsen HJM, Tissing WJE. Substantial decreases in the number and diversity of microbiota during chemotherapy-induced gastrointestinal mucositis in a rat model. Support Care Cancer 2015; 23: 1513–22.

37. Bergman EN. Energy contributions of volatile fatty acids from the gastrointestinal tract in various species. Physiol Rev 1990; 70: 567–90.

38. Giles GI, Jacob C. Reactive sulfur species: an emerging concept in oxidative stress. Biol Chem 2002; 383: 375–88.

39. Ashoori M, Saedisomeolia A. Riboflavin (vitamin B2) and oxidative stress: a review. Br J Nutr 2014; 000: 1–7.

40. Mytilineou C, Kramer BC, Yabut JA. Glutathione depletion and oxidative stress. Parkinsonism Relat Disord 2002; 8: 385–7.

41. Reedquist KA, Tak PP. Signal transduction pathways in chronic inflammatory autoimmune disease: small GTPases. Open Rheumatol J 2012; 6: 259–72.

42. Lakhdari O, Tap J, Béguet-Crespel F, et al. Identification of NF-κB modulation capabilities within human intestinal commensal bacteria. J Biomed Biotechnol 2011; 2011: 282356.

43. Khokhlova EV, Smeianov VV, Efimov BA, Kafarskaia LI, Pavlova SI, Shkoporov AN. Anti-inflammatory properties of intestinal Bifidobacterium strains isolated from healthy infants. Microbiol Immunol 2012; 56: 27–39.

44. Riedel C-U, Foata F, Philippe D, Adolfsson O, Eikmanns B-J, Blum S. Anti-inflammatory effects of bifidobacteria by inhibition of LPS-induced NF-kappaB activation. World J Gastroenterol 2006; 12: 3729–35.

45. Segain JP, Raingeard de la Blétière D, Bourreille A, et al. Butyrate inhibits inflammatory responses through NFkappaB inhibition: implications for Crohn's disease. Gut 2000; 47: 397–403.

46. Wang Y, Xiang G-S, Kourouma F, Umar S. Citrobacter rodentium-induced NF-kappaB activation in hyperproliferating colonic epithelia: role

of p65 (Ser536) phosphorylation. Br J Pharmacol 2006; 148: 814–24.

47. Garrett WS, Gallini CA, Yatsunenko T, et al. Enterobacteriaceae act in concert with the gut microbiota to induce spontaneous and maternally transmitted colitis. Cell Host Microbe 2010; 8: 292–300.

48. Naik SR, Rupawalla EN, Sheth UK. Anti-inflammatory activity of thiamine and nicotinic acid. Biochem Pharmacol 1970; 19: 2867–73.

49. Moallem SA, Hosseinzadeh H, Farahi S. A study of acute and chronic anti-nociceptive and anti-inflammatory effects of thiamine in mice. Iran Biomed J 2008; 12: 173–8.

50. Verhasselt V, Buelens C, Willems F, De Groote D, Haeffner-Cavaillon N, Goldman M. Bacterial lipopolysaccharide stimulates the production of cytokines and the expression of costimulatory molecules by human peripheral blood dendritic cells: evidence for a soluble CD14-dependent pathway. J Immunol 1950; 1997: 2919–25.

51. Carneiro-Filho BA, Lima IPF, Araujo DH, et al. Intestinal barrier function and secretion in methotrexate-induced rat intestinal mucositis. Dig Dis Sci 2004; 49: 65–72.

52. Russo F, Linsalata M, Clemente C, et al. The effects of fluorouracil, epirubicin, and cyclophosphamide (FEC60) on the intestinal barrier function and gut peptides in breast cancer patients: an observational study. BMC Cancer 2013; 13: 56.

53. Nejdfors P, Ekelund M, Weström BR, Willén R, Jeppsson B. Intestinal permeability in humans is increased after radiation therapy. Dis Colon Rectum 2000; 43: 1582–7; discussion 1587–1588.

54. Melichar B, Zezulová M. The significance of altered gastrointestinal permeability in cancer patients. Curr Opin Support Palliat Care 2011; 5: 47–54.

55. Resta-Lenert S, Barrett KE. Probiotics and commensals reverse TNF-alpha- and IFN-gamma-induced dysfunction in human intestinal epithelial cells. Gastroenterology 2006; 130: 731–46.

56. Strowski MZ, Wiedenmann B. Probiotic carbohydrates reduce intestinal permeability and inflammation in metabolic diseases. Gut 2009; 58: 1044–5.

57. Ewaschuk JB, Diaz H, Meddings L, et al. Secreted bioactive factors from Bifidobacterium infantis enhance epithelial cell barrier function. Am J Physiol Gastrointest Liver Physiol 2008; 295: G1025–34.

58. Canani RB, Costanzo MD, Leone L, Pedata M, Meli R, Calignano A. Potential beneficial effects of butyrate in intestinal and extraintestinal diseases. World J Gastroenterol 2011; 17: 1519–28.

59. Vázquez-Castellanos JF, Serrano-Villar S, Latorre A, et al. Altered metabolism of gut microbiota contributes to chronic immune activation in HIV-infected individuals. Mucosal Immunol 2015; 8: 760–72.

60. Guo S, Al-Sadi R, Said HM, Ma TY. Lipopolysaccharide causes an increase in intestinal tight junction permeability in vitro and in vivo by inducing enterocyte membrane expression and localization of TLR-4 and CD14. Am J Pathol 2013; 182: 375–87.

61. Eutamene H, Theodorou V, Schmidlin F, et al. LPS-induced lung inflammation is linked to increased epithelial permeability: role of MLCK. Eur Respir J 2005; 25: 789–96.

62. Lee H-S, Han S-Y, Ryu K-Y, Kim D-H. The degradation of glycosaminoglycans by intestinal microflora deteriorates colitis in mice. Inflammation 2009; 32: 27–36.

63. Burger-van Paassen N, Vincent A, Puiman PJ, et al. The regulation of intestinal mucin MUC2 expression by short-chain fatty acids: implications for epithelial protection. Biochem J 2009; 420: 211–9.

64. Johansson MEV, Phillipson M, Petersson J, Velcich A, Holm L, Hansson GC. The inner of the two Muc2 mucin-dependent mucus layers in colon is devoid of bacteria. Proc Natl Acad Sci USA 2008; 105: 15064–9.

65. Faure M, Mettraux C, Moennoz D, et al. Specific amino acids increase mucin synthesis and microbiota in dextran sulfate sodium-treated rats. J Nutr 2006; 136: 1558–64.

66. Watanabe T, Ohara S, Miyazawa S, Saigenji K, Hotta K. Augmentative effects of L-cysteine and methylmethionine sulfonium chloride on mucin secretion in rabbit gastric mucous cells. J Gastroenterol Hepatol 2000; 15: 45–52.

67. Watanabe T, Ohara S, Ichikawa T, Saigenji K, Hotta K. Mechanisms for cytoprotection by vitamin U from ethanol-induced gastric mucosal damage in rats. Dig Dis Sci 1996; 41: 49–54.

68. Bergstrom KSB, Kissoon-Singh V, Gibson DL, et al. Muc2 protects against lethal infectious colitis by disassociating pathogenic and commensal bacteria from the colonic mucosa. PLoS Pathog 2010; 6: e1000902.

69. Montassier E, Batard E, Gastinne T, Potel G, de La Cochetière MF. Recent

changes in bacteremia in patients with cancer: a systematic review of epidemiology and antibiotic resistance. *Eur J Clin Microbiol Infect Dis* 2013; **32**: 841–50.

70. Almyroudis NG, Fuller A, Jakubowski A, *et al.* Pre- and post-engraftment bloodstream infection rates and associated mortality in allogeneic hematopoietic stem cell transplant recipients. *Transpl Infect Dis* 2005; **7**: 11–7.

71. Poutsiaka DD, Price LL, Ucuzian A, Chan GW, Miller KB, Snydman DR. Blood stream infection after hematopoietic stem cell transplantation is associated with increased mortality. *Bone Marrow Transplant* 2007; **40**: 63–70.

72. Mikulska M, Del Bono V, Raiola AM, *et al.* Enterococcal bloodstream infection after hematopoietic stem cell transplant: experience of a center with a low prevalence of vancomycin-resistant enterococci. *Clin Infect Dis* 2012; **55**: 1744.

73. Blennow O, Ljungman P, Sparrelid E, Mattsson J, Remberger M. Incidence, risk factors, and outcome of bloodstream infections during the pre-engraftment phase in 521 allogeneic hematopoietic stem cell transplantations. *Transpl Infect Dis* 2014; **16**: 106–14.